Journal of Sound and Vibration (1999) **228**(2), 333–358
Article No. jsvi.1999.2410, available online at http://www.idealibrary.com on IDEAL®

THE NON-LINEAR FREE VIBRATION OF FULLY CLAMPED RECTANGULAR PLATES: SECOND NON-LINEAR MODE FOR VARIOUS PLATE ASPECT RATIOS

M. EL KADIRI AND R. BENAMAR

Ecole Mohammadia d'Ingenieurs, Rabat, Morocco

AND

R. G. WHITE

*Department of Aeronautics and Astronautics, University of Southampton S*017 1*BJ, England*

(*Received* 13 *July* 1998, *and in final form* 26 *May* 1999)

The theoretical model based on Hamilton's principle and spectral analysis, previously used to obtain the first three non-linear modes of a clamped–clamped beam [1], and the first non-linear mode of a fully clamped rectangular plate [2], is used here in order to calculate the second non-linear mode of a fully clamped rectangular plate. The large vibration amplitude problem, reduced to a set of non-linear algebraic equations, is solved numerically. Results are given for the second mode of fully clamped rectangular plates, for various plate aspect ratios and vibration amplitudes. The non-linear mode shows a higher bending stress near to the clamps at large deflections, compared with that predicted by linear theory.

1. INTRODUCTION

In spite of the considerable amount of research which has been carried out during the last few decades on non-linear vibration, linear theories remain widely used in most of the practical applications, particularly in the field of modal testing. This seems to be due to the fact that no equivalent has yet been found to the general linear formulation in which the normal modes of free vibration of a structure, with their associated frequencies, play an important role, and facilitate simple expression of the response of a structure in the forced case. Although such a "nonlinear modal analysis theory" has still to be developed, the analogy with the linear case suggests commencing with determination of the non-linear mode shapes and their associated frequencies for structures having a simple geometry. The present work concerned with the second non-linear mode of fully clamped rectangular plates, is a continuation of a series of papers investigating the non-linear modes of beams, homogeneous and composite plates, with various boundary conditions [1–3].

0022-460X/99/470333 + 26 $30.00/0

Determination of the natural frequencies and mode shapes of vibrating plates has been a subject of numerous experimental and theoretical investigations for nearly two centuries, since the experimental work of Chladni was produced in 1787, giving the first known observations of the nodal patterns for completely free square plates [4]. Since then, well-known investigators, such as Rayleigh, Voight, Love and Ritz, have been associated with this problem [4, 5]. However, as the partial differential equation governing the transverse vibrations of thin elastic plates has no complete analytical solution, as pointed out by Love and Timoshenko [5], no exact solutions have yet been found for most of the boundary condition cases. Consider the case of rectangular plates; 21 combinations of classical boundary conditions exist and exact solutions are known only for the six cases having two opposite edges simply supported. Furthermore, in a survey made by Leissa in 1973 [4], it was pointed out that until 1954, when Warburton derived his formulae based on a single-term representation of the deflection mode shapes for the natural frequencies of plates with various boundary conditions, no solution, even approximate, was known for six boundary condition cases. The general accuracy of Warburton's formulae is discussed in reference [4].

Large vibration amplitudes of plate-type structures are encountered in many engineering applications, especially in the aerospace field. Generally, the plates are assumed to be fully or partially free, simply supported or clamped. The clamped support conditions assume that both displacements and rotations are prevented. This is difficult to achieve in practice [6]. However, these boundary conditions can be the most adequate for idealizing practical structures, such as aircraft wing panels [7]. Although in such a situation, the real plate boundaries are neither perfectly clamped nor simply supported, due to the relative support flexibility, the natural frequencies and the stresses calculated on the basis of the fully clamped boundaries assumption are higher than those obtained in the simply supported boundaries case, and hence they may be considered by the designer as an upper limit.[1] Although in the case of fully clamped rectangular plate, the boundary conditions are mathematically simple, compared with the simply supported or free boundaries, there is no exact analytical solution. Even in the linear case, approximate numerical methods, like finite difference techniques, the Galerkin technique, Weinstein's method, integral equations and series methods have been used in the literature to study the linear mode shapes and natural frequencies of fully clamped rectangular plates. A comprehensive treatment of the linear problem and references corresponding to all the above-mentioned methods are given in the monograph of Leissa [9] and in the more recent review mentioned above. A detailed presentation of a series method, based on a Levy-type solution and the superposition theorem is given in reference [10]. The Rayleigh–Ritz method has been adopted in the study of the linear problem in references [11–13]. Although a large number of studies have been carried out on non-linear plate vibrations, as mentioned above, each problem has received a special treatment involving some particular approximations. Some

[1] This is true in the linear case. However, the rate of increase of resonance frequencies, due to the geometrical non-linearity, may be higher in the simply supported case, compared with the clamped–clamped case, as pointed out in reference [8].

of the models available, such as those proposed in references [14, 15], are based on the perturbation procedure, and consequently, are practically limited to the first order effects of finite displacements upon natural frequency. Also, in most of the studies carried out on non-linear vibrations of rectangular plates, the common approach to such problems has been to assume a spatial function, usually the linear mode shape, and seek a solution for the time variable, assuming that the space and time functions can be separated. In a recent series of papers, a theoretical model, based on Hamilton's principle and spectral analysis has been developed for analyzing the dependence of the mode shapes and their corresponding frequencies on the amplitude of vibration for thin straight structures. This approach has been applied to clamped–clamped beams and permitted calculation of the three first non-linear modes and their corresponding frequencies as functions of the vibration amplitude [1]. More recently, several methods such as invariant manifold and perturbation methods, and the method of multiple scales were used to construct the non-linear mode shapes and natural frequencies of one-dimensional continuous systems with weak cubic geometric and inertia non-linearities [16]. Although one-dimensional continuous systems, such as beams, are very useful as theoretical and experimental test pieces, engineering interest is concerned mainly with panel-type structures [17]. The model mentioned above has therefore also been applied to fully clamped rectangular homogeneous and composite plates, leading to the calculation of the first non-linear mode for various values of aspect ratio [2]. However, because of the numerical difficulty of the plate case, which involves two variable functions, obtained as products of x and y beam functions, and requires the use of a greater number of basic functions, compared with the beam case, higher non-linear plate modes have not been treated in the above reference. The purpose of the present work has been calculation of the second non-linear mode of a fully clamped rectangular plate for various values of aspect ratio, and to analyze the effect of non-linearity on the induced bending stresses. Detailed tables of numerical results and plots of the non-linear bending stress corresponding to the non-linear second mode for various amplitudes of vibration and plate sections are given. These numerical data may be easily used in engineering applications. Data concerning the third and higher non-linear modes of rectangular plates will be presented in the future.

2. GENERAL FORMULATION

The purpose of the present paper is to apply the theory developed in reference [2] to the calculation of the second non-linear mode shape of a rectangular plate for various values of the plate aspect ratio and the amplitude of vibration. In this section, a brief review of the theory is presented. The notation used is that defined in reference [2]. Consider the transverse vibrations of a fully clamped rectangular plate having a bending stiffness D,

$$D = \frac{EH^3}{12(1 - \nu^2)}. \tag{1}$$

For such a plate, the strain energy V is given as the sum of the strain energy due to bending (V_b) and the membrane strain energy induced by large deflections (V_a): $V = V_a + V_b$, with

$$V_b = \frac{1}{2}\int_S D\left(\frac{\partial^2 W}{\partial x^2} + \frac{\partial^2 W}{\partial y^2}\right)^2 \mathrm{d}S \tag{2}$$

and

$$V_a = \frac{3D}{2H^2}\int_S \left[\left(\frac{\partial W}{\partial x}\right)^2 + \frac{\partial W}{\partial y}\right)^2\Big]^2 \mathrm{d}S, \tag{3}$$

in which W is the deflection function and S the plate area. In the above expression, terms involving the in-plane displacements U and V and their derivatives have been omitted. This assumption has been made in reference [2] when calculating the first non-linear mode of fully clamped rectangular plates and its range of validity has been discussed in the light of the experimental and numerical results obtained for the frequency amplitude dependence and the bending stress estimates obtained at large vibrations amplitudes. The results obtained via this assumption were compared with the previous ones based on various methods such as the finite element method, the method based on Berger's approximation, the ultraspherical polynomial method and the elliptic function method. It was found that the percentage error in the non-linear frequency estimates based on this assumption, for amplitudes up to 1·5 times the thickness, does not exceed 1·3%. Also, in the experimental investigation of the non-linear behaviour of fully clamped rectangular plates at large vibration amplitudes presented in reference [18], it was found that the rate of increase in bending stresses estimates, obtained from measured data, was in a very good agreement with that obtained from the theory, in which the assumption of zero in-plane displacements was made. Hence, it is thought that such a conclusion may justify this assumption, which induces a great simplification in the model and a great reduction in the computation time, when calculating the non-linear modes and the associated frequencies and non-linear bending stresses patterns for a reasonable range of vibrations amplitudes and plates aspect ratios. However, further investigations are needed, which should take into account the in-plane displacements U and V, in order to examine the effects of large vibration amplitudes on the axial stress patterns for fully clamped rectangular plates.

The kinetic energy T of the plate is

$$T = \frac{1}{2}\rho H \int_S \left(\frac{\partial W}{\partial t}\right)^2 \mathrm{d}S. \tag{4}$$

The transverse displacement function W is expanded as a series of n basic functions:

$$W = a_i(x, y)W_i(t) = a_i(x, y)\sin \omega t, \tag{5}$$

where the usual summation convention for repeated indexes is used. Assuming that the time and space functions are separable and that harmonic motion takes place,

one obtains after discretization of the above expressions,

$$T = \tfrac{1}{2}\omega^2 a_i a_j m_{ij} \cos^2(\omega t), \tag{6}$$

$$V_b = \tfrac{1}{2}\sin^2(\omega t)\, a_i a_j k_{ij}; \tag{7}$$

$$V_a = \tfrac{1}{2}\, a_i a_j a_k a_l b_{ijkl} \sin^4(\omega t), \tag{8}$$

where m_{ij} k_{ij} and b_{ijkl} are the mass tensor, the rigidity tensor and the non-linearity tensor respectively. The expressions for these tensors are given in reference [2]. Applying Hamilton principle to the vibration problem gives

$$\delta \int_0^{2\pi/\omega} (V - T)\, \mathrm{d}t = 0. \tag{9}$$

Replacing T and V in this equation by their expressions given above, integrating the time functions and calculating the derivatives with respect to the a_is leads to the following set of non-linear algebraic equations:

$$3a_i a_j a_k\, b^*_{ijkr} + 2a_i\, k^*_{ir} - 2a_i \omega^{2*} m^*_{ir} = 0, \quad r = 1, \ldots, n \tag{10}$$

which have to be solved numerically. In order to complete the formulation the procedure adopted in the present paper is similar to that developed in reference [2] to obtain the fundamental non-linear mode. It is based on use of the equation $V_{\max} = T_{\max}$ in order to obtain the $(n+1)$th equation necessary for calculating the $(n+1)$ unknowns, i.e., the a_i's ($i = 1$–n) and ω^*. This leads to the following equation:

$$\omega^{2*} = \frac{a_i a_j k^*_{ij} + a_i a_j a_k a_l\, b^*_{ijkl}}{a_i a_j m^*_{ij}}, \tag{11}$$

which has to be substituted in equations (10) to obtain a system of n nonlinear algebraic equations leading to the n contribution coefficients a_i, $i = 1$–n. The contribution of the basic function corresponding to the second mode is first fixed, and other basic function contributions are calculated via numerical solution of the remaining $(n-1)$ non-linear algebraic equations as in reference [2]. The Harwell library routine NS01A used in reference [2] to obtain the first non-linear mode has been successfully used here to obtain the numerical results presented for the second non-linear mode.

3. SECOND NON-LINEAR MODE SHAPE

3.1. NUMERICAL DETAIL

Consider the fully clamped rectangular plate, shown in Figure (1), whose aspect ratio $\alpha = b/a$, is less than 1. For such a plate, the deflections in the x and y directions are represented here by clamped–clamped beam functions. These functions, which satisfy all the fully clamped theoretical boundary conditions, i.e., zero displacement and zero slope along the four plate edges, have been used and shown to be appropriate in previous studies of the vibration of fully clamped rectangular plates [1, 2, 4, 6]. In the remainder of this paper, the simple index i used in the series expansion of the plate deflection function W, i.e., equation (5), is replaced by

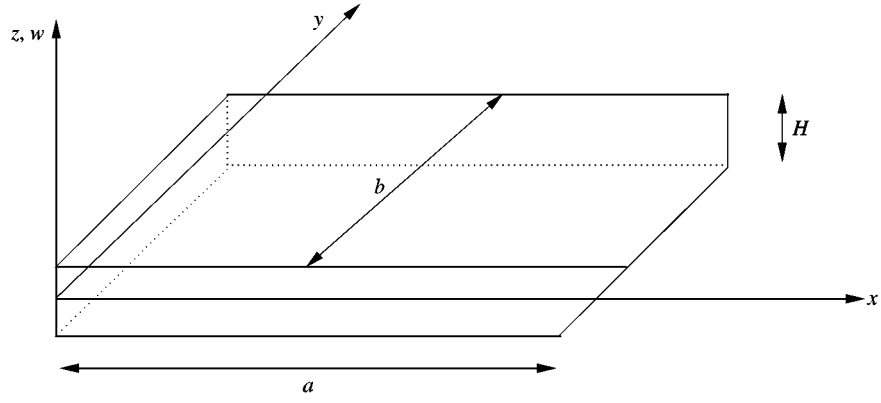

Figure 1. Plate notation.

a double index *ij*:

$$a_k(x, y) = \alpha_{ij} W_{ij}(x, y), \tag{12}$$

where α_{ij} is the influence coefficient of product of the *i*th and *j*th beam mode shapes on the *k*th non-linear mode of vibration. The analytical expressions and the shapes of the clamped–clamped beam functions are given in reference [2]. The fundamental non-linear mode shape of a fully clamped rectangular thin elastic plate is symmetric in both the x and y directions. To calculate it, 25 basic functions obtained as products of the first five clamped–clamped beam mode shapes were used, which involve three symmetric beam functions in each direction.

Consider now the second linear mode shape of the plate. As $\alpha = b/a$ is less than 1, it is antisymmetric in the x direction and symmetric in the y direction. Previous studies have shown that only nine plate functions corresponding to three antisymmetric beam functions in the x direction and three symmetric beam functions in the y direction contribute significantly to this mode [4, 9, 12]. These nine plate functions involve the first six beam functions. Use of all of the first six beam functions for both the x and y directions would have led to 36 plate functions and hence to the solution of 35 non-linear algebraic equations involving $36^4 = 1\,679\,616$ terms of the non-linear rigidity tensor b_{ijkl}. Because of such unnecessary numerical difficulty, due to the fact that only plate functions antisymmetric in the x direction and symmetric in the y direction were expected to contribute to the second non-linear mode shape, calculations were made using only the nine plate functions satisfying the above conditions of symmetry among the 36 functions obtained as products of the first six beam functions. This led to a set of eight non-linear algebraic equations which has been solved numerically for various values of the amplitude of vibration and plate aspect ratios. The routine used is based on a hybrid method combining the steepest descent and Newton's methods and consequently exploits the advantages of both methods [19]. A step procedure, similar to that described in references [1, 2], was adopted for ensuring rapid convergence when varying the amplitude, which allowed solutions to be obtained with a quite reasonable number of iterations (an average of 80 for eight equations).

However, the number of iterations necessary here for ensuring convergence was much higher than that needed when calculating the first non-linear mode (30 iterations for 24 equations) [2].

3.2. TYPICAL VALUES OBTAINED BY USE OF 25 FUNCTIONS

To confirm the good convergence of the series expansion and the validity of use of only the nine plate functions mentioned in the above section, the second non-linear plate mode shape has also been calculated using 25 plate functions obtained as product of the first five beam functions (symmetric and antisymmetric), and an example of the numerical results obtained for a square plate and non-dimensional vibration amplitudes of 0·1157, 0·6742 and 3·1928 are listed in Table 1. It can be seen that functions having significant contributions are those expected according to the analysis given above, i.e., a_{21}, a_{41}, a_{23}, a_{43}, a_{25} and a_{45}. The values of their contributions, listed in Table 1, are very close to those corresponding to the same functions in Table 2, in which results obtained using only nine well-chosen plate functions are given. The slight difference is due to the

TABLE 1

Second non-linear mode shape of a fully clamped square plate: typical numerical results obtained with 25 basic functions

W^*_{max}	0·1157	0·6742	3·1928
$\omega nl^*/\omega l^*$	1·0047	1·1453	2·7190
a_{11}	0·3963E − 10	− 0·3270E − 09	− 0·1548E − 08
a_{21}	0·05	0·3	1·5
a_{31}	− 0·6584E − 11	0·4967E − 11	0·1362E − 09
a_{41}	0·5915E − 03	0·1526E − 01	0·1923E + 00
a_{51}	0·2003E − 10	0·4541E − 11	0·9316E − 10
a_{12}	0·1173E − 09	0·2213E − 13	0·8671E − 15
a_{22}	− 0·3377E − 10	− 0·2011E − 09	− 0·9420E − 09
a_{32}	0·4209E − 12	0·8494E − 13	− 0·5349E − 15
a_{42}	− 0·9203E − 11	− 0·1231E − 10	− 0·1236E − 09
a_{52}	− 0·3193E − 11	− 0·1719E − 12	0·7077E − 15
a_{13}	− 0·1716E − 10	− 0·2956E − 10	− 0·2611E − 09
a_{23}	0·2119E − 02	0·2444E − 01	0·2673E + 00
a_{33}	0·4902E − 10	0·1359E − 11	0·7211E − 10
a_{43}	− 0·1102E − 03	− 0·5962E − 03	0·2424E − 01
a_{53}	− 0·6135E − 11	− 0·2635E − 11	− 0·5692E − 10
a_{14}	− 0·1686E − 11	− 0·1150E − 12	0·1355E − 15
a_{24}	0·2561E − 11	− 0·2018E − 10	− 0·1706E − 09
a_{34}	0·1420E − 10	0·1513E − 14	0·1153E − 14
a_{44}	− 0·2133E − 10	− 0·6841E − 12	− 0·2067E − 10
a_{54}	− 0·5461E − 12	− 0·7982E − 13	0·2394E − 15
a_{15}	0·1933E − 10	− 0·3300E − 11	− 0·6349E − 10
a_{25}	0·3540E − 03	0·3239E − 02	0·6355E − 01
a_{35}	− 0·1568E − 10	− 0·6188E − 13	0·2282E − 10
a_{45}	− 0·5090E − 04	− 0·1812E − 03	0·4256E − 02
a_{55}	0·1726E − 11	0·1471E − 12	− 0·3424E − 10

TABLE 2

Contribution coefficients to the second non-linear mode shape of a fully clamped rectangular plate $\alpha = 1$

w^*_{max}	$\omega nl/\omega l$	a_{21}	a_{23}	a_{25}	a_{41}	a_{43}	a_{45}	a_{61}	a_{63}	a_{65}
0·115701	1·0047	0·05	0·2113E − 02	0·3519E − 03	0·5947E − 03	− 0·1132E − 03	− 0·5301E − 04	0·9161E − 04	− 0·3093E − 04	− 0·2570E − 04
0·230510	1·0185	0·10	0·4693E − 02	0·7307E − 03	0·1681E − 02	− 0·2435E − 03	− 0·1005E − 03	0·1303E − 03	− 0·2712E − 04	− 0·5533E − 04
0·343826	1·0406	0·15	0·8091E − 02	0·1169E − 02	0·3603E − 02	− 0·3851E − 03	− 0·1396E − 03	0·8772E − 04	0·3702E − 04	− 0·8870E − 04
0·455558	1·0698	0·20	0·1250E − 01	0·1706E − 02	0·6510E − 02	− 0·5048E − 03	− 0·1704E − 03	− 0·3366E − 04	0·1753E − 03	− 0·1201E − 03
0·565507	1·1049	0·25	0·1797E − 01	0·2380E − 02	0·1039E − 01	− 0·5554E − 03	− 0·1930E − 03	− 0·2108E − 03	0·3930E − 03	− 0·1398E − 03
0·674169	1·1451	0·30	0·2447E − 01	0·3226E − 02	0·1515E − 01	− 0·4910E − 03	− 0·2059E − 03	− 0·4137E − 03	0·6910E − 05	− 0·1360E − 03
0·781590	1·1896	0·35	0·3188E − 01	0·4268E − 02	0·2063E − 01	− 0·2775E − 03	− 0·2057E − 03	− 0·6148E − 03	0·1069E − 02	− 0·9707E − 04
0·887857	1·2377	0·40	0·4008E − 01	0·5520E − 02	0·2672E − 01	0·1047E − 03	− 0·1879E − 03	− 0·7933E − 03	0·1525E − 02	− 0·1269E − 04
0·993711	1·2889	0·45	0·4894E − 01	0·6984E − 02	0·3328E − 01	0·6609E − 03	− 0·1475E − 03	− 0·9352E − 03	0·2058E − 02	0·1252E − 03
1·09897	1·3428	0·50	0·5834E − 01	0·8656E − 02	0·4019E − 01	0·1386E − 02	− 0·8054E − 04	− 0·1033E − 02	0·2665E − 02	0·3220E − 03
1·20373	1·3991	0·55	0·6815E − 01	0·1052E − 01	0·4738E − 01	0·2267E − 02	0·1583E − 04	− 0·1084E − 02	0·3344E − 02	0·5808E − 03
1·41249	1·5179	0·65	0·8864E − 01	0·1477E − 01	0·6229E − 01	0·4427E − 02	0·3008E − 03	− 0·1048E − 02	0·4901E − 02	0·1286E − 02
1·62143	1·6435	0·75	0·1098E + 00	0·1956E − 01	0·7762E − 01	0·6999E − 02	0·7037E − 03	− 0·8524E − 03	0·6691E − 02	0·2226E − 02
1·83024	1·7747	0·85	0·1313E + 00	0·2475E − 01	0·9312E − 01	0·9850E − 02	0·1208E − 02	− 0·5303E − 03	0·8669E − 02	0·3370E − 02
2·03914	1·9103	0·95	0·1529E + 00	0·3021E − 01	0·1087E + 00	0·1288E − 01	0·1793E − 02	− 0·1149E − 03	0·1079E − 01	0·4682E − 02
2·24821	2·0497	1·05	0·1745E + 00	0·3583E − 01	0·1242E + 00	0·1602E − 01	0·2437E − 02	0·3662E − 03	0·1303E − 01	0·6126E − 02
3·19281	2·7090	1·50	0·2702E + 00	0·6181E − 01	0·1928E + 00	0·3046E − 01	0·5699E − 02	0·2897E − 02	0·2376E − 01	0·1352E − 01
4·24634	3·4778	2·00	0·3738E + 00	0·9035E − 01	0·2673E + 00	0·4616E − 01	0·9461E − 02	0·5824E − 02	0·3594E − 01	0·2225E − 01

TABLE 3

Comparison of contribution coefficients to the second mode shape of a fully clamped square plate: $\alpha = 1{\cdot}0$ (a) *results from linear analysis, reference* [12]; (b) *present results obtained from non-linear analysis for* $w^* = 0{\cdot}1157$

$\omega l^* \; \omega nl^*$	a_{21}	a_{23}	a_{25}	a_{41}	a_{43}	a_{45}	a_{61}	a_{63}	a_{65}
(a) 73·41	1	0·0406	0·0070	0·0101	−0·0022	−0·0011	0·0020	−0·0007	−0·0005
(b) 73·76	1	0·0423	0·0070	0·0119	−0·0023	−0·0011	0·0018	−0·0006	−0·0005

TABLE 4

Comparison of contribution coefficients to the second mode shape of a fully clamped square plate: $\alpha = 0{\cdot}8$ (a) *linear results calculated here*; (b) *present results obtained from non-linear analysis for* $w^* = 0{\cdot}1174$

$\omega l \; \omega nl^*$	a_{21}	a_{23}	a_{25}	a_{41}	a_{43}	a_{45}	a_{61}	a_{63}	a_{65}
(a) 52·523	1	0·0296	0·0047	0·0153	−0·00258	−0·00093	0·00313	−0·00108	−0·00053
(b) 52·745	1	0·0305	0·0047	0·0169	−0·00260	−0·00091	0·00298	−0·00095	−0·00055

TABLE 5

Comparison of contribution coefficients to the second mode shape of a fully clamped square plate: $\alpha = 0{\cdot}2$ (a) *linear results calculated here*; (b) *present results obtained from non-linear analysis for* $w^* = 0{\cdot}1131$

$\omega l \; \omega nl^*$	a_{21}	a_{23}	a_{25}	a_{41}	a_{43}	a_{45}	a_{61}	a_{63}	a_{65}
(a) 23·447	1	0·0024	0·0003	0·097	−0·00006	−0·00001	0·0297	−0·0003	−0·00004
(b) 23·509	1	0·0026	0·0004	0·095	−0·00005	−0·000002	0·0327	−0·00027	−0·00007

fact that the 25 functions used do not involve the functions W_{61}, W_{63} and W_{65} which contribute to the second non-linear mode shape, as shown in Table 2.

3.3. COMPARISON OF SOLUTIONS OBTAINED FROM THE NON-LINEAR MODEL AT SMALL AMPLITUDES WITH LINEAR SOLUTIONS

In Tables 3–5, numerical solutions of the set of non-linear algebraic equations corresponding to the non-linear vibration problem, obtained for $a_{21} = 0{\cdot}05$ are compared with results given by Leissa in reference [9] from Rayleigh–Ritz analysis of the linear problem, for plates having aspect ratios of 1, 0·8 and 0·2 respectively. It can be seen that both resonance frequencies and contribution coefficients obtained from the non-linear analysis at small vibration amplitudes are very close to those obtained from the linear analysis. Also, in Table 6(a), non-linear frequency parameters obtained here from the non-linear analysis for small values of a_{21} are compared with parameters obtained from previous linear analyses [20–22]

TABLE 6(a)

Comparison of non-dimensional frequency parameters: (*a*) *linear results calculated here*: (*b*) *non-linear results obtained here for small amplitudes* ($a_{21} = 0{\cdot}05$) (*corresponding to* $W^* = 0{\cdot}1158$ *for* $\alpha = 1$ *for example*) *and various aspect ratios*

Aspect ratio α	0·2	0·4	0·6	0·8	1
$\omega l^*(a)$	23·447	27·816	37·277	52·523	73·40
$\omega nl^*(b)$	23·509	27·895	37·407	52·745	73·76

TABLE 6(b)

Comparison of non-dimensional frequency parameters, corresponding to various plate aspect ratios: (*a*) *linear results obtained in reference* [20]; (*b*) *linear results obtained in reference* [21]; (*c*) *linear results obtained in reference* [22]; (*d*) *non-linear results obtained here for very small amplitudes* ($a_{21} = 0{\cdot}005$ *corresponding to* $W^* = 0{\cdot}01158$ *when* $\alpha = 1$)

Aspect ratio α	0·4	0·66	1	1·5	2·0	2·5
ωl^*(a)	27·81	41·73	73·41	93·87		173·84
ωl^*(b)			73·413	93·86		
ωl^*(c)			73·3947		127·307	
ωnl^*(d)	27·82	41·72	73·416	93·86	127·348	173·88

corresponding to various plate aspect ratios. In Table 6(b) non-linear frequency parameters obtained here from the non-linear analysis for very small values of a_{21} are compared with parameters obtained from the solution of the eigenvalue problem for other values of the plate aspect ratio. In both Tables 6(a) and (b), corresponding to various plate aspect ratios, very good agreement can be seen between data from a linear model and the non-linear model at small deflections. It is worth noting here, from the numerical methods point of view, that a classical eigenvalue problem, solved usually by using classical numerical methods, such as Jacobi's method, appears here, as has been pointed out when dealing with the first non-linear plate mode shape in reference [2], as a limit of a non-linear problem, described by a set of non-linear algebraic equations, the solution of which tends to the eigenvalue problem solution when the displacement amplitude tends to zero.

3.4. COMPARISON OF THE AMPLITUDE FREQUENCY DEPENDENCE CALCULATED VIA THE PRESENT THEORY WITH PREVIOUS RESULTS

In order to estimate the accuracy of the results obtained by the present theory and the effects of the approximations adopted, a comparison has been made with

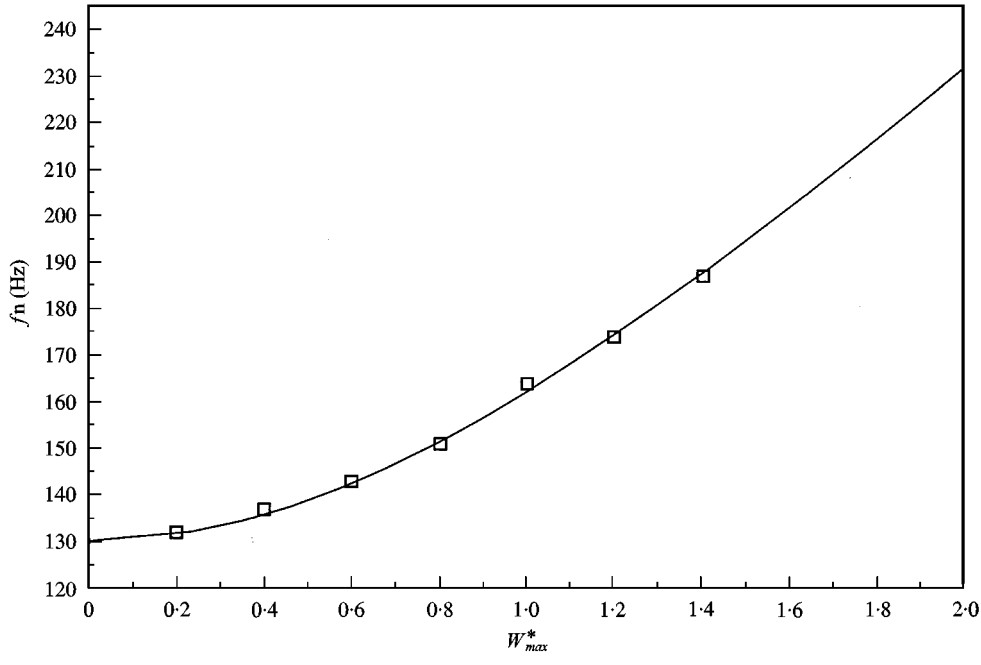

Figure 2. Comparison of non-linear resonant frequency of the 2nd mode of an isotropic plate $\alpha = 2/3$. □ values taken from [23], read from graph; — present work.

previous results. Most of the available results for fully clamped rectangular plates are concerned with the first non-linear mode. Only one reference has been found in which the non-linear resonant frequency of the second mode of an isotropic rectangular plate (aspect ratio = 2/3), calculated using the hierarchical finite element method was presented. Figure 2 shows very good agreement between results given in reference [23] and the results calculated via the present model. This good agreement, added to the reasons mentioned in Section 2, shows that the assumption of zero in-plane displacements made in equation (2) can lead to good estimation of the second non-linear mode of fully clamped rectangular plates.

4. GENERAL PRESENTATION OF NUMERICAL RESULTS

Numerical results corresponding to assigned values of a_{21} varying from 0·05 to 2 corresponding to a maximum displacement amplitude to thickness ratio varying from 0·1131 to 4·942, obtained at $(x^*, y^*) = (0{\cdot}5, 0{\cdot}25)$, and $\alpha = 0{\cdot}2, 0{\cdot}4, 0{\cdot}6, 0{\cdot}8$ and 1, are summarized in Tables 2, 7–10. In each table, a_{ij} represents the contribution of the basic function obtained as product of the ith and jth x and y clamped–clamped beam functions, $w^*_{\max}$ is the maximum non-dimensional amplitude and ω^*_{nl}/ω^*_l is the ratio of the non-linear non-dimensional frequency parameter defined in equation (11) to the linear non-dimensional frequency parameter obtained by diagonalization of the linear system.

TABLE 7

Contribution coefficients to the second non-linear mode shape of a fully clamped rectangular plate $\alpha = 0{\cdot}2$

w^*_{max}	$\omega nl/\omega l$	a_{21}	a_{23}	a_{25}	a_{41}	a_{43}	a_{45}	a_{61}	a_{63}	a_{65}
0·113120	1·0027	0·05	0·1320E − 03	0·2135E − 04	0·4769E − 02	− 0·2269E − 05	0·1106E − 06	0·1636E − 02	− 0·1327E − 04	− 0·3803E − 05
0·228566	1·0104	0·10	0·3421E − 03	0·7957E − 04	0·9242E − 02	− 0·5704E − 06	0·3525E − 05	0·4106E − 02	− 0·1489E − 04	− 0·1572E − 04
0·347453	1·0229	0·15	0·6957E − 03	0·2079E − 03	0·1339E − 01	0·8625E − 05	0·1261E − 04	0·7942E − 02	0·7844E − 05	− 0·4060E − 04
0·469659	1·0397	0·20	0·1239E − 02	0·4341E − 03	0·1738E − 01	0·2834E − 04	0·2909E − 04	0·1328E − 01	0·6852E − 04	− 0·7886E − 04
0·594445	1·0604	0·25	0·2002E − 02	0·7804E − 03	0·2135E − 01	0·6110E − 04	0·5460E − 04	0·1993E − 01	0·1803E − 03	− 0·1276E − 03
0·720949	1·0846	0·30	0·2997E − 02	0·1264E − 02	0·2537E − 01	0·1087E − 03	0·9073E − 04	0·2760E − 01	0·3546E − 03	− 0·1824E − 03
0·848423	1·1119	0·35	0·4225E − 02	0·1898E − 02	0·2946E − 01	0·1723E − 03	0·1389E − 03	0·3597E − 01	0·5998E − 03	− 0·2385E − 03
0·976303	1·1419	0·40	0·5679E − 02	0·2689E − 02	0·3362E − 01	0·2521E − 03	0·2002E − 03	0·4477E − 01	0·9212E − 03	− 0·2915E − 03
1·10420	1·1744	0·45	0·7341E − 02	0·3641E − 02	0·3783E − 01	0·3477E − 03	0·2752E − 03	0·5382E − 01	0·1321E − 02	− 0·3377E − 03
1·23188	1·2091	0·50	0·9192E − 02	0·4754E − 02	0·4209E − 01	0·4582E − 03	0·3643E − 02	0·6300E − 01	0·1799E − 02	− 0·3740E − 03
1·35920	1·2457	0·55	0·1121E − 01	0·6024E − 02	0·4637E − 01	0·5824E − 03	0·4674E − 03	0·7223E − 01	0·2352E − 02	− 0·3977E − 03
1·61252	1·3239	0·65	0·1565E − 01	0·9010E − 02	0·5502E − 01	0·8658E − 03	0·7142E − 03	0·9065E − 01	0·3666E − 02	− 0·3991E − 03
1·86405	1·4075	0·75	0·2049E − 01	0·1253E − 01	0·6374E − 01	0·1186E − 02	0·1011E − 02	0·1089E + 00	0·5219E − 02	− 0·3292E − 03
2·11436	1·4954	0·85	0·2560E − 01	0·1651E − 01	0·7250E − 01	0·1534E − 02	0·1350E − 02	0·1270E + 00	0·6961E − 02	− 0·1810E − 03
2·36334	1·5869	0·95	0·3088E − 01	0·2086E − 01	0·8128E − 01	0·1899E − 02	0·1726E − 02	0·1449E + 00	0·8843E − 02	0·4770E − 04
2·61124	1·6813	1·05	0·3627E − 01	0·2551E − 01	0·9007E − 01	0·2277E − 02	0·2130E − 02	0·1626E + 00	0·1083E − 01	0·3549E − 03
3·71842	2·1325	1·50	0·6086E − 01	0·4861E − 01	0·1297E + 00	0·4030E − 02	0·4168E − 02	0·2415E + 00	0·2029E − 01	0·2543E − 02
4·94160	2·6662	2·00	0·8788E − 01	0·7576E − 01	0·1735E + 00	0·5971E − 02	0·6588E − 02	0·3278E + 00	0·3093E − 01	0·5916E − 02

TABLE 8

Contribution coefficients to the second non-linear mode shape of a fully clamped rectangular plate $\alpha = 0{\cdot}4$

w^*_{max}	$\omega nl/\omega l$	a_{21}	a_{23}	a_{25}	a_{41}	a_{43}	a_{45}	a_{61}	a_{63}	a_{65}
0·115639	1·0028	0·05	0·4697E − 03	0·6688E − 04	0·2426E − 02	− 0·6198E − 04	− 0·1132E − 04	0·5792E − 03	− 0·5579E − 04	− 0·1518E − 04
0·230778	1·0112	0·10	0·1036E − 02	0·1684E − 03	0·5149E − 02	− 0·1151E − 03	− 0·2022E − 04	0·1256E − 02	− 0·8347E − 04	− 0·4005E − 04
0·345077	1·0248	0·15	0·1784E − 02	0·3372E − 03	0·8378E − 02	− 0·1507E − 03	− 0·2369E − 04	0·2118E − 02	− 0·5538E − 04	− 0·8301E − 04
0·458410	1·0433	0·20	0·2778E − 02	0·6015E − 03	0·1221E − 01	− 0·1606E − 03	− 0·1804E − 04	0·3227E − 02	0·5487E − 04	− 0·1503E − 04
0·570820	1·0663	0·25	0·4058E − 02	0·9845E − 03	0·1663E − 01	− 0·1383E − 03	0·8537E − 06	0·4619E − 02	0·2712E − 03	− 0·2453E − 03
0·682430	1·0934	0·30	0·5643E − 02	0·1504E − 02	0·2158E − 01	− 0·7960E − 04	0·3689E − 04	0·6300E − 02	0·6137E − 03	− 0·3690E − 03
0·793379	1·1240	0·35	0·9714E − 02	0·2990E − 02	0·3266E − 01	0·1517E − 03	0·1725E − 03	0·1044E − 01	0·1734E − 02	− 0·6915E − 03
0·903978	1·1578	0·40	0·5679E − 02	0·2689E − 02	0·3362E − 01	0·2521E − 03	0·2002E − 03	0·4477E − 01	0·9212E − 03	− 0·2915E − 03
1·01425	1·1943	0·45	0·1216E − 01	0·3966E − 02	0·3862E − 01	0·3213E − 03	0·2757E − 03	0·1284E − 01	0·2526E − 02	− 0·8905E − 03
1·12420	1·2333	0·50	0·1485E − 01	0·5094E − 02	0·4477E − 01	0·5224E − 03	0·4032E − 03	0·1540E − 01	0·3475E − 02	− 0·1102E − 02
1·23387	1·2744	0·55	0·1776E − 01	0·6370E − 02	0·5105E − 01	0·7507E − 03	0·5545E − 03	0·1810E − 01	0·4576E − 02	− 0·1324E − 02
1·45250	1·3609	0·65	0·2409E − 01	0·9332E − 02	0·6385E − 01	0·1272E − 02	0·9233E − 03	0·2377E − 01	0·7204E − 02	− 0·1783E − 02
1·67066	1·4557	0·75	0·3096E − 01	0·1278E − 01	0·7680E − 01	0·1852E − 02	0·1369E − 02	0·2968E − 01	0·1033E − 02	− 0·2239E − 02
1·88874	1·5540	0·85	0·3821E − 01	0·1662E − 01	0·8979E − 01	0·2466E − 02	0·1875E − 02	0·3572E − 01	0·1386E − 01	− 0·2668E − 02
2·10636	1·6561	0·95	0·4570E − 01	0·2079E − 01	0·1027E + 00	0·3097E − 02	0·2425E − 02	0·4182E − 01	0·1770E − 01	− 0·3056E − 02
2·32360	1·7615	1·05	0·5336E − 01	0·2521E − 01	0·1156E + 00	0·3733E − 02	0·3008E − 02	0·4795E − 01	0·2178E − 01	− 0·3397E − 02
3·30094	2·2636	1·50	0·8854E − 01	0·4683E − 01	0·1729E + 00	0·6552E − 02	0·5798E − 02	0·7538E − 01	0·4158E − 01	− 0·4339E − 02
4·38552	2·8554	2·00	0·1275E + 00	0·7129E − 01	0·2353E + 00	0·9537E − 02	0·8911E − 02	0·1054E + 00	0·6414E − 01	− 0·4603E − 02

TABLE 9

Contribution coefficients to the second non-linear mode shape of a fully clamped rectangular plate $\alpha = 0{\cdot}6$

w^*_{max}	$\omega nl/\omega l$	a_{21}	a_{23}	a_{25}	a_{41}	a_{43}	a_{45}	a_{61}	a_{63}	a_{65}
0·116951	1·0035	0·05	0·9592E − 03	0·1404E − 03	0·1345E − 02	− 0·1188E − 03	− 0·3003E − 04	0·2691E − 03	− 0·6280E − 04	− 0·2482E − 04
0·232905	1·0138	0·10	0·2073E − 02	0·3112E − 03	0·3108E − 02	− 0·2313E − 03	− 0·5638E − 04	0·5291E − 03	− 0·8882E − 04	− 0·5781E − 04
0·347148	1·0305	0·15	0·3475E − 02	0·5416E − 03	0·5588E − 02	− 0·3275E − 03	− 0·7535E − 04	0·7843E − 03	− 0·4413E − 04	− 0·1055E − 03
0·459498	1·0530	0·20	0·5260E − 02	0·8580E − 03	0·8924E − 02	− 0·3940E − 03	− 0·8329E − 04	0·1055E − 02	0·1005E − 03	− 0·1715E − 03
0·569933	1·0807	0·25	0·7488E − 02	0·1283E − 02	0·1311E − 01	− 0·4162E − 03	− 0·7670E − 04	0·1368E − 02	0·3688E − 03	− 0·2566E − 03
0·678659	1·1130	0·30	0·1018E − 01	0·1834E − 02	0·1805E − 01	− 0·3811E − 03	− 0·5243E − 04	0·1749E − 02	0·7788E − 03	− 0·3583E − 03
0·785952	1·1493	0·35	0·1333E − 01	0·2524E − 02	0·2362E − 01	− 0·2800E − 03	− 0·7929E − 05	0·2218E − 02	0·1343E − 02	− 0·4720E − 03
0·892088	1·1890	0·40	0·1691E − 01	0·3359E − 02	0·2970E − 01	− 0·1087E − 03	0·5854E − 04	0·2781E − 02	0·2068E − 02	− 0·5918E − 03
0·997705	1·2317	0·45	0·2088E − 01	0·4341E − 02	0·3615E − 01	0·1327E − 03	0·1479E − 03	0·3441E − 02	0·2956E − 02	− 0·7109E − 03
1·10271	1·2772	0·50	0·2519E − 01	0·5470E − 02	0·4289E − 01	0·4409E − 03	0·2601E − 03	0·4193E − 02	0·4004E − 02	− 0·8229E − 03
1·20720	1·3249	0·55	0·2981E − 01	0·6739E − 02	0·4984E − 01	0·8106E − 03	0·3945E − 03	0·5029E − 02	0·5207E − 02	− 0·9218E − 03
1·41526	1·4263	0·65	0·3974E − 01	0·9670E − 02	0·6413E − 01	0·1708E − 02	0·7244E − 03	0·6920E − 02	0·8035E − 02	− 0·1061E − 02
1·62326	1·5342	0·75	0·5037E − 01	0·1306E − 01	0·7869E − 01	0·2770E − 02	0·1124E − 02	0·9041E − 02	0·1135E − 01	− 0·1100E − 02
1·83068	1·6473	0·85	0·6145E − 01	0·1682E − 01	0·9335E − 01	0·3947E − 02	0·1577E − 02	0·1133E − 01	0·1506E − 01	− 0·1027E − 02
2·03815	1·7646	0·95	0·7280E − 01	0·2088E − 01	0·1080E + 00	0·5200E − 02	0·2069E − 02	0·1373E − 01	0·1907E − 01	− 0·8426E − 03
2·24604	1·8853	1·05	0·8430E − 01	0·2517E − 01	0·1226E + 00	0·6501E − 02	0·2588E − 02	0·1621E − 01	0·2331E − 01	− 0·5543E − 03
3·18189	2·4590	1·50	0·1365E + 00	0·4599E − 01	0·1873E + 00	0·1254E − 01	0·5045E − 02	0·2775E − 01	0·4373E − 01	0·1698E − 02
4·22402	3·1314	2·00	0·1936E + 00	0·6994E − 01	0·2576E + 00	0·1913E − 01	0·7756E − 02	0·4058E − 01	0·6697E − 01	0·5111E − 02

TABLE 10

Contribution coefficients to the second non-linear mode shape of a fully clamped rectangular plate $\alpha = 0{\cdot}8$

w^*_{max}	$\omega nl/\omega l$	a_{21}	a_{23}	a_{25}	a_{41}	a_{43}	a_{45}	a_{61}	a_{63}	a_{65}
0·117414	1·0042	0·05	0·1527E − 02	0·2373E − 03	0·8499E − 03	− 0·1303E − 03	− 0·4559E − 04	0·1429E − 03	− 0·4768E − 04	− 0·2769E − 04
0·233690	1·0166	0·10	0·3328E − 02	0·5014E − 03	0·2167E − 02	− 0·2657E − 03	− 0·8605E − 04	0·2581E − 03	− 0·5834E − 04	− 0·6135E − 04
0·348017	1·0365	0·15	0·5628E − 02	0·8197E − 02	0·4285E − 02	− 0·3993E − 03	− 0·1175E − 03	0·3074E − 03	− 0·8811E − 06	− 0·1043E − 03
0·460030	1·0631	0·20	0·8571E − 02	0·1220E − 02	0·7351E − 02	− 0·5102E − 03	− 0·1374E − 03	0·3044E − 03	0·1474E − 03	− 0·1555E − 03
0·569927	1·0954	0·25	0·1223E − 01	0·1729E − 02	0·1136E − 01	− 0·5693E − 03	− 0·1441E − 03	0·2739E − 03	0·4014E − 03	− 0·2102E − 03
0·677996	1·1326	0·30	0·1661E − 01	0·2367E − 02	0·1620E − 01	− 0·5480E − 03	− 0·1361E − 03	0·2454E − 03	0·7707E − 03	− 0·2606E − 03
0·784406	1·1740	0·35	0·2168E − 01	0·3152E − 02	0·2175E − 01	− 0·4243E − 03	− 0·1116E − 03	0·2442E − 03	0·1260E − 02	− 0·2970E − 03
0·889741	1·2190	0·40	0·2738E − 01	0·4094E − 02	0·2786E − 01	− 0·1847E − 03	0·6880E − 04	0·2885E − 03	0·1872E − 02	− 0·3097E − 03
0·994314	1·2672	0·45	0·3363E − 01	0·5195E − 02	0·3441E − 01	0·1756E − 03	− 0·6359E − 05	0·3885E − 03	0·2605E − 02	− 0·2894E − 03
1·09807	1·3181	0·50	0·4036E − 01	0·6456E − 02	0·4129E − 01	0·6545E − 03	0·7671E − 04	0·5483E − 03	0·3455E − 02	− 0·2284E − 03
1·20146	1·3714	0·55	0·4749E − 01	0·7870E − 02	0·4841E − 01	0·1245E − 02	0·1808E − 03	0·7677E − 03	0·4417E − 02	− 0·1206E − 03
1·40768	1·4840	0·65	0·6264E − 01	0·1112E − 01	0·6315E − 01	0·2719E − 02	0·4500E − 03	0·1371E − 02	0·6647E − 02	0·2501E − 03
1·61321	1·6034	0·75	0·7862E − 01	0·1484E − 01	0·7825E − 01	0·4506E − 02	0·7933E − 03	0·2159E − 02	0·9227E − 02	0·8343E − 03
1·81886	1·7282	0·85	0·9509E − 01	0·1894E − 01	0·9349E − 01	0·6516E − 02	0·1198E − 02	0·3087E − 02	0·1209E − 01	0·1622E − 02
2·02405	1·8574	0·95	0·1118E + 00	0·2332E − 01	0·1087E + 00	0·8675E − 02	0·1650E − 02	0·4117E − 02	0·1517E − 01	0·2589E − 02
2·23027	1·9903	1·05	0·1287E + 00	0·2790E − 01	0·1240E + 00	0·1093E − 01	0·2137E − 02	0·5217E − 02	0·1840E − 01	0·3708E − 02
3·15923	2·6193	1·50	0·2041E + 00	0·4965E − 01	0·1914E + 00	0·2146E − 01	0·4529E − 02	0·1054E − 01	0·3394E − 01	0·9912E − 02
4·19482	3·3539	2·00	0·2862E + 00	0·7410E − 01	0·2646E + 00	0·3300E − 01	0·7247E − 02	0·1652E − 01	0·5156E − 01	0·1767E − 01

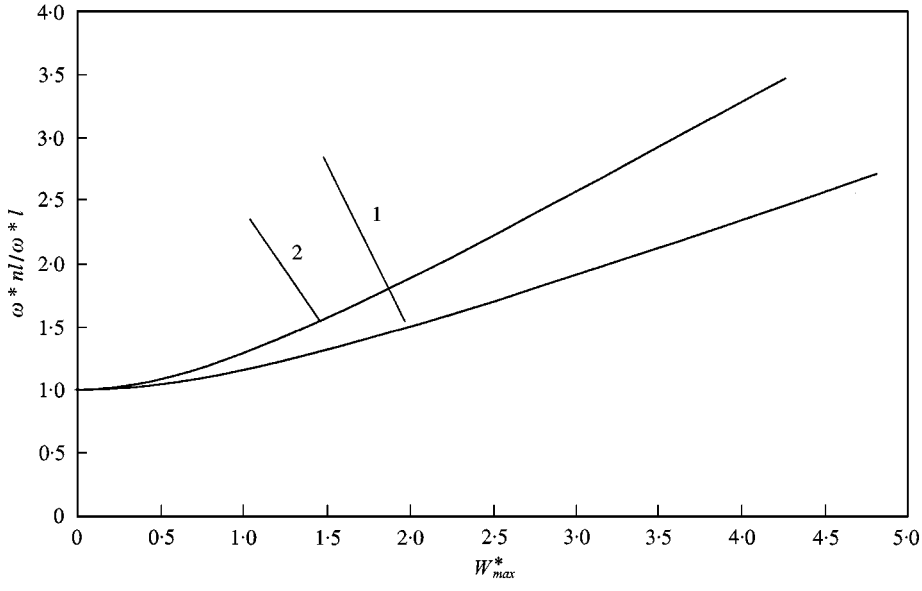

Figure 3. Comparison of the change in natural frequency for the first and the 2nd mode (square plate $\alpha = 1$). Curve 1: first non-linear mode; Curve 2: second non-linear mode.

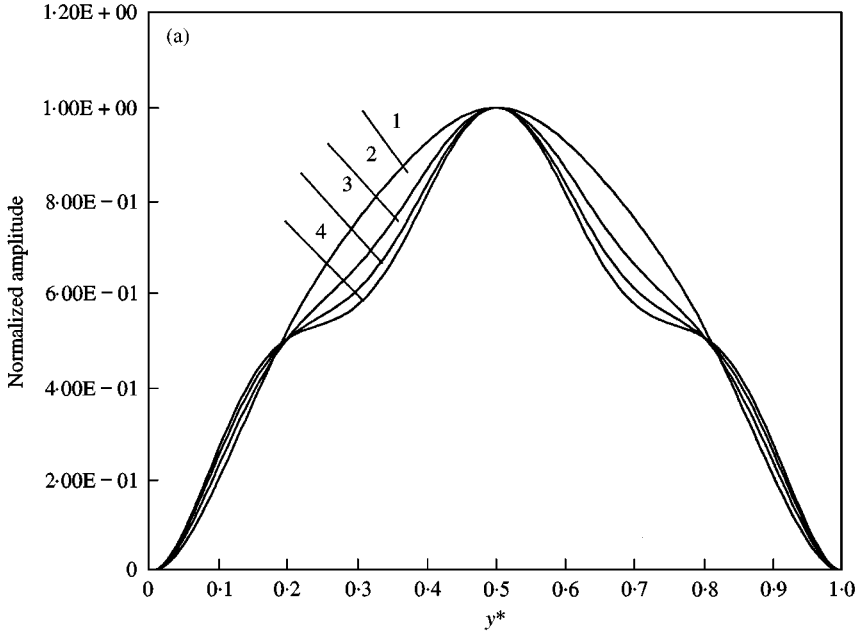

Figure 4(a). Normalized second non-linear mode rectangular plate $\alpha = 0{\cdot}2$, $x^* = 0{\cdot}025$. Curve 1: lowest amplitude; Curve 4: highest amplitude.

5. AMPLITUDE DEPENDENCE OF THE SECOND MODE SHAPE

The dependence of the non-linear frequency on the amplitude of vibration is plotted in Figure 3, for both the first and second mode of a fully clamped square

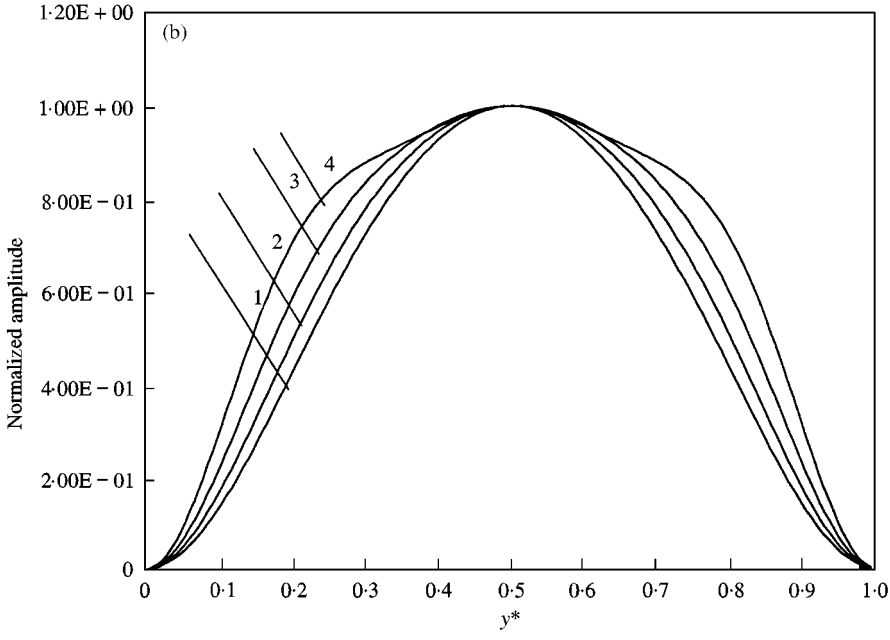

Figure 4(b). Normalized second non-linear mode square plate $\alpha = 1$, $x^* = 0{\cdot}025$. Curve 1: lowest amplitude; Curve 4: highest amplitude.

TABLE 11

Maximum displacement amplitude W^*_{max} corresponding to the normalized curves given in Figures 4–13

W^*	Aspect ratio α	1	0·8	0·6	0·4	0·2
	Curve 1	0·115701	0·117414	0·116951	0·115639	0·113120
	Curve 2	0·674169	0·677996	0·678659	0·682430	0·720949
	Curve 3	1·20373	1·20146	1·20720	1·23387	1·35920
	Curve 4	2·24821	2·23027	2·24604	2·32360	2·61124

plate ($\alpha = 1$), with the ratio of non-linear frequency $\omega^* nl$ against the maximum non-dimensional amplitude w^*_{max}. The curves of Figure 3 show that the first non-linear mode exhibits less change in frequency with amplitude than does the second non-linear mode. This fact is not surprising, since for the same maximum displacement amplitude, the deflection shape associated with the first mode produces less induced tension than that associated with the second mode. In Figures 4(a) and (b) normalized symmetric sections of the non-linear second mode shape corresponding to $x^* = 0{\cdot}025$ and $\alpha = 0{\cdot}2$ and 1, are plotted for the values of the maximum non-dimensional amplitudes given in Table 11. All curves show the amplitude dependence of symmetric sections of the second mode shape. They show that the non-linear mode shapes in the neighbourhood of the clamps can be very different from those expected in the linear theory. In Figures 5(a) and (b)

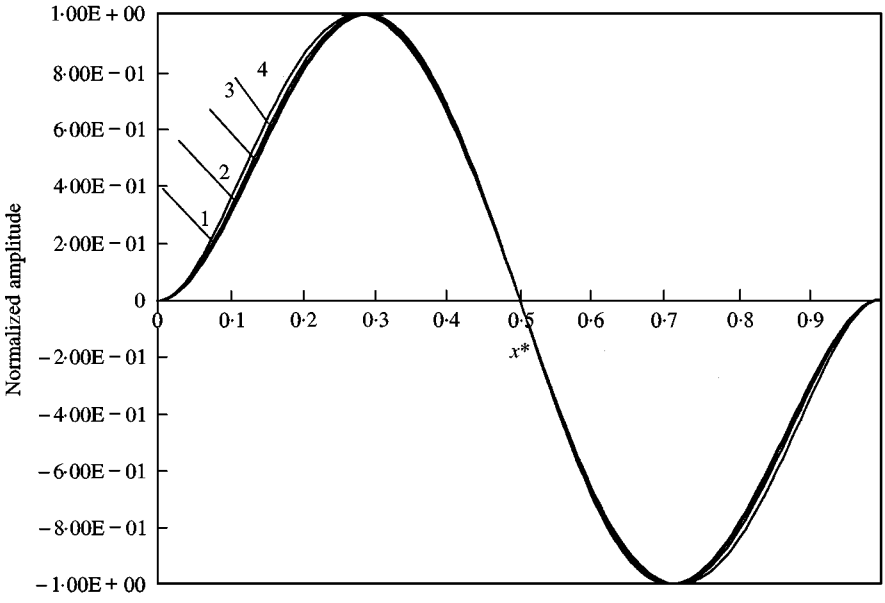

Figure 5(a). Normalized second non-linear mode rectangular plate $\alpha = 0{\cdot}2$, $y^* = 0{\cdot}025$. Curve 1: lowest amplitude; Curve 4: highest amplitude.

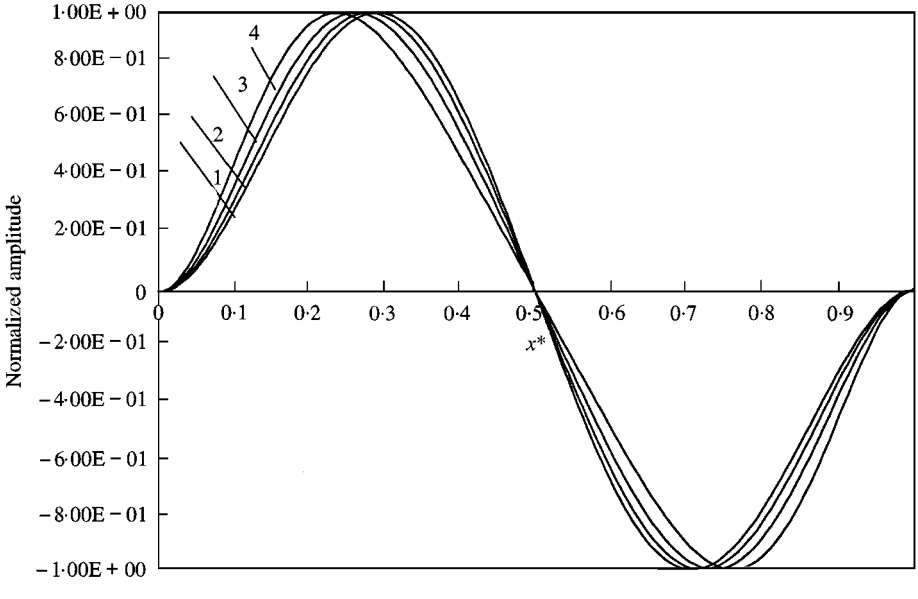

Figure 5(b). Normalized second non-linear mode rectangular plate $\alpha = 0{\cdot}6$, $y^* = 0{\cdot}025$. Curve 1: lowest amplitude; Curve 4: highest amplitude.

normalized antisymmetric plots of the non-linear second mode shape corresponding to $y^* = 0{\cdot}025$ and $\alpha = 0{\cdot}2$; 0·6 are presented for the values of the maximum non-dimensional amplitudes w^*_{max} given in Table 11. These curves show that antisymmetric components of the second non-linear mode shape are also amplitude dependent with an increase of curvature near to the clamps and a displacement of

the maximum amplitude towards the clamps, as has been pointed out in reference [1] for the second non-linear mode shape of a clamped–clamped beam.

6. BENDING STRESSES ASSOCIATED WITH THE SECOND NON-LINEAR MODE SHAPE

The maximum bending strain ε_{xb} and ε_{yb} obtained for $z = H/2$ are given by

$$\varepsilon_{xb} = \frac{H}{2}\left(\frac{\partial^2 w}{\partial x^2}\right), \quad \varepsilon_{yb} = \frac{H}{2}\left(\frac{\partial^2 w}{\partial y^2}\right). \tag{13–14}$$

By using the classical thin plate assumption of plane stress and Hooke's law, the stresses can be obtained as

$$\sigma_{xb} = \frac{EH}{2(1-v^2)}\left(\left(\frac{\partial^2 w}{\partial x^2}\right) + v\left(\frac{\partial^2 w}{\partial y^2}\right)\right), \tag{15}$$

$$\sigma_{yb} = \frac{EH}{2(1-v^2)}\left(\left(\frac{\partial^2 w}{\partial y^2}\right) + v\left(\frac{\partial^2 w}{\partial x^2}\right)\right). \tag{16}$$

In terms of the non-dimensional parameters defined in reference [2], non-dimensional stresses σ^*_{xb} and σ^*_{yb} can be defined by

$$\sigma^*_{xb} = \left(\frac{\partial^2 w^*}{\partial x^{*2}}\right) + v\left(\frac{\partial^2 w^*}{\partial y^{*2}}\right), \tag{17}$$

$$\sigma^*_{yb} = \left(\frac{\partial^2 w^*}{\partial y^{*2}}\right) + v\,\alpha^2\left(\frac{\partial^2 w^*}{\partial x^{*2}}\right). \tag{18}$$

The relationships between the dimensional and non-dimensional stresses are

$$\sigma = \frac{EH^2}{2(1-v^2)}\sigma^*, \tag{19}$$

which is valid for both dimensional and non-dimensional pairs of stresses defined in equations (15–18).

The non-dimensional bending stress distribution associated with the rectangular plate second non-linear mode is plotted in Figure 6 for $x^* = 0{\cdot}025$ and $\alpha = 1$. It can be seen in this figure, corresponding to a region which is very close to the clamps, that the bending stress can exhibit a quite unusual distribution, with a positive bending stresses along the whole section parallel to the y direction, i.e., the symmetric direction of the second mode. Such a non-linear effect has been mentioned in reference [2] for the plate non-linear fundamental mode and was attributed to the Poisson's ratio effect and to high curvatures in the other direction (i.e. the x direction in the present case). The non-dimensional bending stress distribution, associated with the second non-linear mode, is plotted for various plate aspect ratios and various sections parallel to directions of symmetry and antisymmetry of the mode in Figures 7(a, b) and (8a, b). All curves show the amplitude dependence of the stress distribution, and a high increase of the bending stress near to the clamps, compared with the rate of increase expected in the linear theory. Table 12 summarizes some numerical data concerning the rate of increase in bending stresses. The non-dimensional bending stress at the point $A(x^* = 0{\cdot}025,$

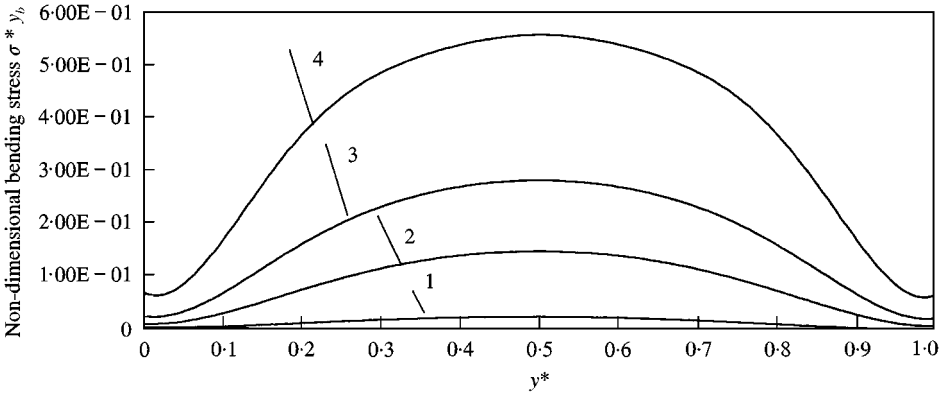

Figure 6. Non-dimensional bending stress distribution associated with the fully clamped rectangular plate second non-linear mode for $\alpha = 1$ along the section $x^* = 0{\cdot}025$. Curve 1: lowest amplitude; Curve 4: highest amplitude.

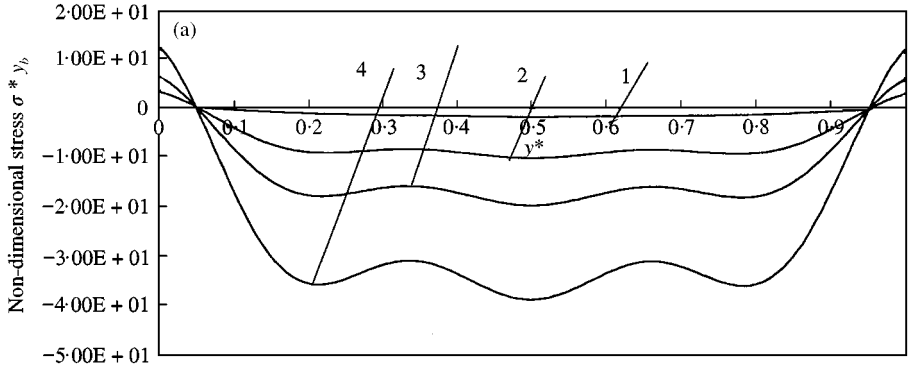

Figure 7(a). Non-dimensional bending stress distribution associated with the fully clamped rectangular plate second non-linear mode for $\alpha = 0{\cdot}2$ along the section $x^* = 0{\cdot}25$. Curve 1: lowest amplitude; Curve 4: highest amplitude.

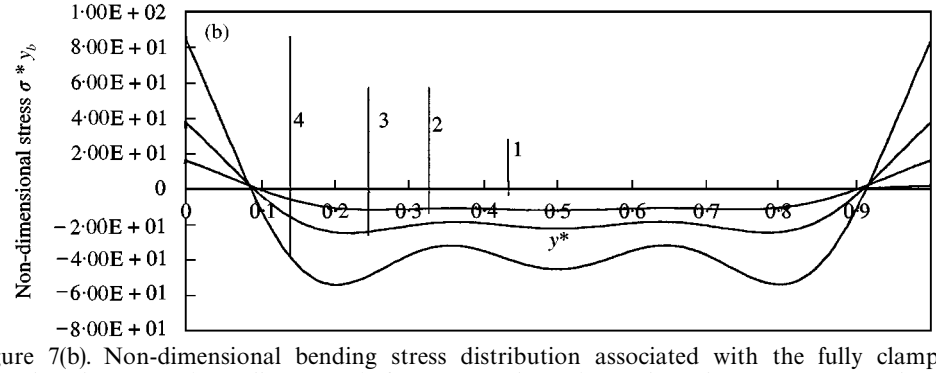

Figure 7(b). Non-dimensional bending stress distribution associated with the fully clamped rectangular plate second non-linear mode for $\alpha = 0{\cdot}6$ along the section $x^* = 0{\cdot}25$. Curve 1: lowest amplitude; Curve 4: highest amplitude.

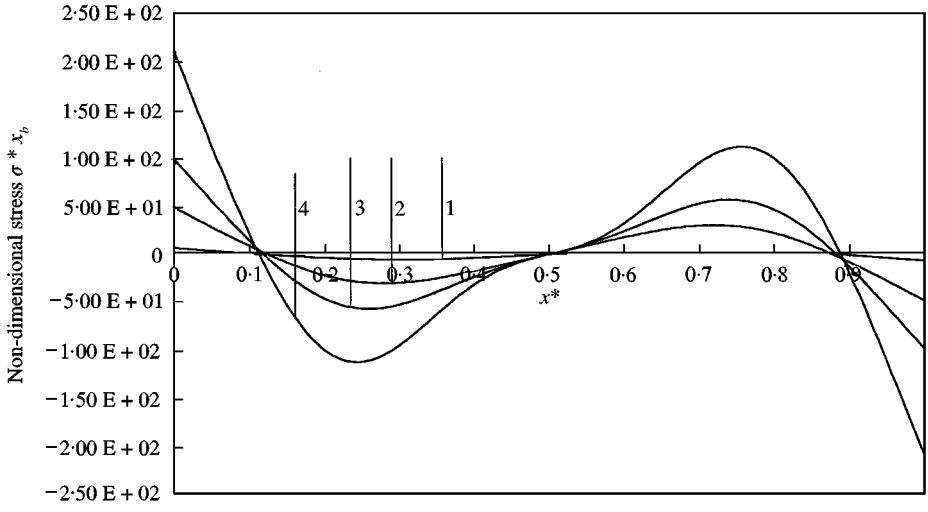

Figure 8(a). Non-dimensional bending stress distribution associated with the fully clamped rectangular plate second non-linear mode for $\alpha = 0{\cdot}2$ along the section $y^* = 0{\cdot}25$. Curve 1: lowest amplitude; Curve 4: highest amplitude.

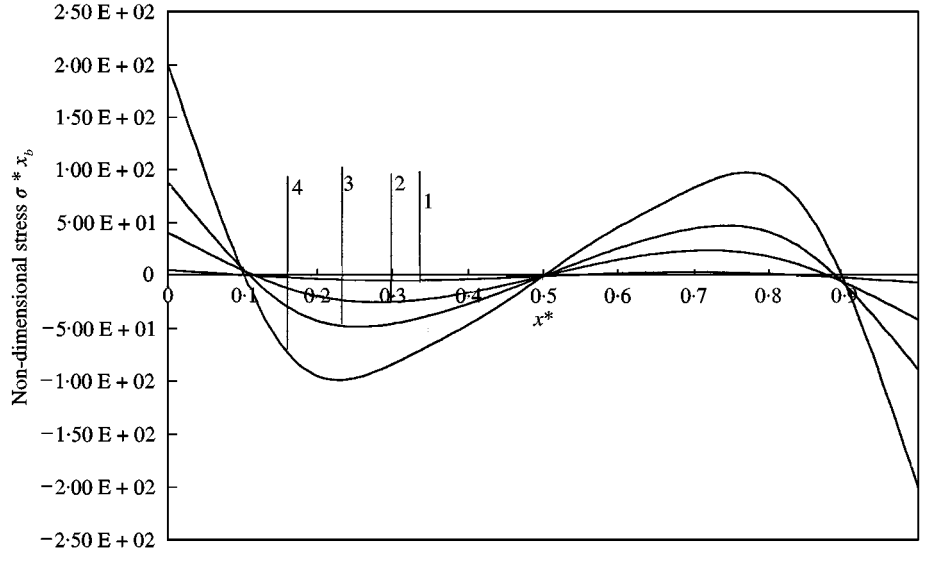

Figure 8(b). Non-dimensional bending stress distribution associated with the fully clamped rectangular plate second non-linear mode for $\alpha = 1$ along the section $y^* = 0{\cdot}25$. Curve 1: lowest amplitude; Curve 4: highest amplitude.

$y^* = 0{\cdot}025$) of a plate corresponding to $\alpha = 0{\cdot}6$, increases from 0·067 to 3·95, when the non-dimensional amplitude increases from 0·1169 to 2·2460, as indicated in Table 12. This is about three times the increase expected in the linear theory.

7. CONCLUSIONS

The non-linear model developed in references [1, 2] for non-linear free vibrations of thin elastic structures occurring at large displacement amplitudes has been

TABLE 12

Comparison of the rate of increase of the non-dimensional bending stress σ^* x_b *with increasing* $w^*_{\max}$ *at various points*: *A*: $(x^*, y^*) = (0, 025; 0, 025)$; *B*: (0, 25; 0, 025), *C*: (0, 5; 0, 025); *D*: (0, 025; 0, 25); $R(w^*)$: *Rate of increase of* $w^*_{\max}$; $R(\sigma^* xb)$; *Rate of increase of* $\sigma^* x_b$. *The reference value is the first value. Rectangular plate* $\alpha = 0{\cdot}6$

$\omega nl^*/\omega l^*$	$w^*_{\max}$	$R(W^*)$	$\sigma^*(A)$	$R(\sigma^*(A))$	$\sigma^*(B)$	$R(\sigma^*(B))$	$\sigma^*(C)$	$R(\sigma^*(C))$	$\sigma^*(D)$	$R(\sigma^*(D))$
1·0035	0·11695		0·0679		1·44		2·26		1·49	
1·3249	1·2072	10·322272	1·57	23·122239	21·9	15·208333	26·5	11·725664	27·6	18·52349
1·8853	2·24604	19·204966	3·95	58·173785	46·8	32·5	54	23·893805	60·7	40·738255

successfully used in the present work to determine numerically the amplitude dependence of the second non-linear mode shape of fully clamped rectangular plates, for various aspect ratios and vibration amplitudes, via the solution of a set of non-linear algebraic equations, involving a fourth order tensor due to the geometrical non-linearity. The amplitude-dependent second non-linear mode shape was expressed as a series of plate functions obtained as products of clamped–clamped x and y beam functions. As was expected, it was noticed that plate functions obtained using higher order beam functions, compared with those used for the first non-linear mode in reference [2], contribute significantly to the second non-linear mode. Consequently, the size of the tensors increased and the process of solution became quite long. However, a convergence study showed that only plate functions representing the shape of the second mode (antisymmetric in the x-direction and symmetric in the y-direction) have a significant contribution to the second non-linear mode. This justified the use of only nine well-chosen plate functions, which made the numerical solution much easier to obtain.

Considering the results obtained, numerical data corresponding to various values of the plate aspect ratio and amplitudes of vibration up to 4·94 times the plate thickness are given. Plots of the amplitude-dependent plate second mode showed clearly that the geometrical non-linearity induces a deformation of the mode, in both the symmetric and antisymmetric directions, with a displacement of the extremum line towards the clamps when the amplitude increases. As a consequence of the deformation of the mode, it was shown that the rate of increase in the induced bending stresses in a region close to the clamps can be three times higher than that expected in the linear theory.

It appears from the present work that the non-linear model developed in references [1, 2] allows higher order non-linear fully clamped rectangular plate modes to be quite easily estimated and can be considered as an extension of the classical linear eigen value problem for free vibration of plates. It shows also qualitatively and quantitatively how it can be inaccurate to assume linear mode shapes when expressing the non-linear response of plate structures. Further investigations are needed in order to allow higher order modes to be estimated and to find out how the estimated non-linear modes can be simply used in order to express the non-linear forced response for engineering purposes. Also the effects of such a non-linearity on the fatigue life of highly excited plate-type structures has to be investigated. There is considerable relevance to the acoustic fatigue problem in aircraft structures.

REFERENCES

1. R. Benamar, M. M. K. Bennouna and R. G. White 1991 *Journal of Sound and Vibration* **149**, 179–195. The effects of large vibration amplitudes on the fundamental mode shape of thin elastic structures, part I: simply supported and clamped–clamped beams.
2. R. Benamar, M. M. K. Bennouna and R. G. White 1993 *Journal of Sound and Vibration* **164**, 295–316. The effects of large vibration amplitudes on the fundamental mode shape of thin elastic structures, part II: Fully clamped rectangular isotropic plates.

3. R. Benamar, M. M. K. Bennouna and R. G. White 1990 *Fourth International Conference of Recent Advances in Structural Dynamics*, 749–760. The effects of Large Vibration Amplitudes on the Fundamental Mode Shape of a Fully clamped, Symmetrically laminated rectangular plate.
4. A. W. Leissa 1973 *Journal of Sound and Vibration* **31**, 257–393. Free vibrations of rectangular plates.
5. R. F. McLean 1982 *Applied Mathematical Analysis*: *Vibration Theory* (G. F. Roach, editor), 23–55. The biharmonic equation and its finite difference approximations.
6. S. Abrate and G. Schoeppner 1997 29 *International SAMPE* (*Society for the Advancement of Materials and Process Engineering*) *Technical Conference October* 28–*November* 1, *Orlando*, *FL*, 725–732. Identification of support conditions for composite beams and plates from natural frequencies.
7. C. E. Teh 1989 *Ph.D. Thesis*, *Institute of Sound and Vibration Research*. Dynamic behaviour and acoustic fatigue of isotropic and anisotropic panels under combined acoustic excitation and static in plane compression.
8. A. V. Srinivasan 1965 *A.I.A.A Journal* **3**, 1951–1953. Large amplitude-free oscillations of beams and plates.
9. A. W. Leissa 1969 *Vibrations of Plates*, *NASA SP*-160, Washington, D.C. U.S. Government Printing Office.
10. D. J. Gorman 1982 *Free Vibration Analysis of Rectangular Plates*, 69–100. Amsterdam: Elsevier North-Holland, Inc.
11. G. B. Warburton 1954 *Proceedings of the Institution of Mechanical Engineers*, *Series A*. **168**, 371–384. The vibration of rectangular plates.
12. D. Young 1950 *Journal of Applied Mechanics*, 448–453. Vibration of rectangular plates by the Ritz method.
13. J. Nagaraja and S. S. Rao 1953 *Journal of Aeronautical Science* **20**, 855–856. Vibrations of rectangular plates.
14. H. N. Chu and G. Hermann 1956 *Journal of Applied Mechanics* **23**, 532–540. Influence of large amplitudes on free flexural vibrations of rectangular elastic plates.
15. L. W. Rehfield 1973 *International Journal of Solids and Structures* **9**, 581–590. Nonlinear free vibrations of elastic structures.
16. A. H. Nayfeh and S. A. Nayfeh 1994 *Journal of Vibration and Acoustics* **116**, 129–136. On Nonlinear modes of continuous systems.
17. R. G. White 1975 *Journal of the Royal Aeronautical Society* 318–325. Some measurements of the dynamic properties of mixed carbon fibre reinforced, plastic beams and plates.
18. R. Benamar, M. M. K. Bennouna and R. G. White 1994 *Journal of Sound and Vibration* **175**, 377–395. The effects of large vibration amplitudes on the mode shapes and natural frequencies of thin elastic structures, part III: Fully clamped rectangular isotropic plates – Measurements of the mode shape amplitude dependence and the spatial distribution of harmonic distortion.
19. M. J. D. Powell 1965 *Computer Journal* A method for minimising a sum of squares of nonlinear functions without calculating derivatives.
20. K. M. Liew, K. Y. Lam and S. T. Chow 1988 *Computers and Structures* **34**, 79–85. Free vibration analysis of rectangular plates using orthogonal plate function.
21. R. B. Bhat 1985 *Journal of Sound and Vibration* **102**, 493–499. Natural frequencies of rectangular plates using characteristic orthogonal polynomials in the Rayleigh-Ritz method.
22. R. B. Bhat, P. A. A. Laura, R. G. Gutierrez, V. H. Cortinez and H. C. Sanzi 1990 *Journal of Sound and Vibration* **138**, 205–219. Numerical experiments on the determination of natural frequencies of transverse vibrations of rectangular plates of nonuniform thickness.
23. W. Han and M. Petyt 1997 *Computers and Structures* **63**, 309–318. Geoemetrically nonlinear vibration analysis of thin, rectangular plates using the hierarchical finite element methods. II: First mode of laminated plates and higher modes of isotropic and laminated plates.

APPENDIX A: NUMERICAL DETAILS OF THE CLAMPED–CLAMPED BEAM ANALYSIS

The chosen basic functions W_i were the linear clamped–clamped beam functions

$$W_1(x) = \frac{\cosh(v_i x/L) - \cos(v_i x/L)}{\cosh v_i - \cos v_i} - \frac{\sinh(v_i x/L) - \sin(v_i x/L)}{\sinh v_i - \sin v_i}$$

where v_i for $i = 1, 2, \ldots$ are the eigenvalue parameters for a clamped–clamped beam. The values of the parameters V_i were computed by solving numerically the transcendental equation $\cosh v_i \cos v_i = 1$ and are given in Table 13. The functions w_i were normalized in such a manner that

$$m_{ij}^* = \int_0^1 w_1^*(x^*) w_j^*(x^*)\,\mathrm{d}x^* = \delta_{ij}.$$

The functions w_i^*, $i = 1, \ldots, 5$, are shown in Figure 9.

TABLE 13

Symmetric (a) *and antisymmetric* (b) *eigenvalue parameters for a clamped–clamped beam*

	(*a*)		(*b*)
1	4·73004075	2	7·85320462
3	10·99560784	4	14·13716549
5	17·27875966	6	20·42035225
7	23·56194490	8	26·70353756
9	29·84513021	10	32·98672286
11	36·12831552	12	39·26990817

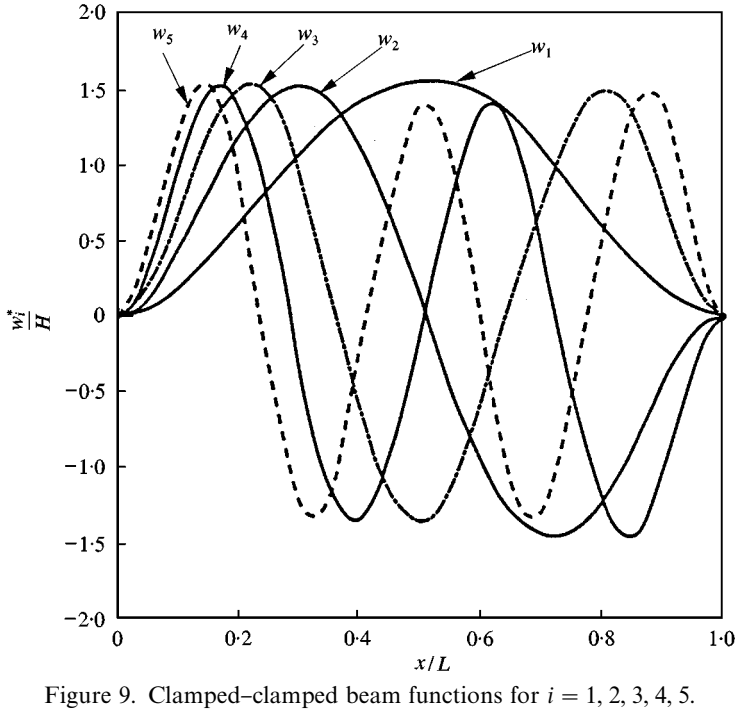

Figure 9. Clamped–clamped beam functions for $i = 1, 2, 3, 4, 5$.

APPENDIX B: NOTATION

a_{ij}	contribution coefficient of the plate deflection function as a product of the ith and jth beam mode shapes in the x and y directions, respectively
a, b	length, width of the plate
E	Young's modulus
H	plate thickness
k_{ij}, m_{ij} and b_{ijkl}	general term of the rigidity tensor, the mass and the non-linearity tensor respectively
k^*_{ij}, m^*_{ij} and b^*_{ijkl}	General term of the non-dimensional rigidity tensor, mass tensor and non-linearity tensor respectively
S, S^*	Dimensional and non-dimensional surfaces $[0, a] \times [0, b]$ and $[0, 1] \times [0, 1]$ respectively
T	kinetic energy
$U(x, y, t)$, $V(x, y, t)$	in-plane displacements at point (x, y) of the plate $U(x, y, t) = u(x, y)\sin^2 \omega t$ $V(x, y, t) = v(x, y)\sin^2 \omega t$
V_b, V_a and V	Bending, axial and total strain energy respectively
$W(x, y, t)$	transverse displacement at point x on the plate $W(x, y, t) = w(x, y)\sin \omega t$
$W^*(x, y, t)$	non-dimensional transverse displacement at point x on the plate
$W^*_{\max}$	maximum of the non-dimensional transverse displacement
x, y	point co-ordinates
α	non-dimensional parameter (aspect ratio) given by $\alpha = b/a$
ν	Poisson's ratio
ρ	mass density per unit volume of the plate
ω, ω^*	frequency and non-dimensional frequency parameter respectively
σ_{xb}, σ_{yb}	Dimensional bending stresses
σ^*_{xb}, σ^*_{yb}	Non-dimensional bending stresses